Engineering Innovations *Online: 2025-02-06*
ISSN: 2813-1002, Vol. 13, pp 57-73
doi:10.4028/p-h2WAGU

Assessing Rainwater Harvesting Potential in Seawater-Based Communities Using the Case Study of Poblacion Sitangkai, Philippines

Marie Fe Y. Lacsado[1,2,a], Doris B. Montecastro[2,3,b]

[1]Department of Civil Engineering and Professional Schools, University of Mindanao, Matina, Davao City 8000, Philippines

[2]School of Engineering and Architecture, Ateneo de Davao University, Davao City, Davao del Sur, Philippines

[3]Environmental Science Department, Ateneo de Davao University, Davao City 8000, Philippines

[a]mfylacsado@addu.edu.ph, [b]dbmontecastro@addu.edu.ph

Keywords: Geographic Information System, Spatial Analysis, Rainfall Data, Rainwater Harvesting Potential, Digitized Roof Area, Vector Grid, Seawater-Based Community.

Abstract. A lack of fresh water is a serious issue in communities near or surrounded by seawater, such as Sitangkai Poblacion, where they rely heavily on the ocean for their water source. QGIS with vector grid as the tool will help to study the possibility of efficient rainwater harvesting. Data processing for analysis of rainfall data from Weatherlink station in Bongao, Tawi-Tawi, and roof area digitization conducted for Sitangkai Poblacion. The spatial distribution of rainwater harvesting was assessed systematically at the 200 m x 200 m vector grid level. Data was collected on monthly precipitation during June 2023 and March 2024 to estimate possible water collection volumes. The results present significant grid-to-grid variability in the potential for rainwater harvesting, driven by roof area and regional rainfall patterns. The months when there was a lot of rainfall during the rainy season are significantly associated with the month peak rainwater harvesting occurred; this means an ideal time to boost water collection. The study demonstrates the necessity of specific rainwater harvesting approaches that focus on dominant household variables in conjunction with improved storage and holistic water handling procedures for sustainable solutions for these areas. Vector grid in QGIS can be a potential methodology for researchers to spatially analyze and guide sustainable water resource planning addressing freshwater scarcity.

Introduction

Due to the scarcity of freshwater sources, many seawater-based communities [1], [2] require solutions for water-related issues since access to this limited supply and its salty nature have created several problems in their daily lives. To address water scarcity, a solution named Rainwater Harvesting (RWH) has rightly come into existence globally, particularly in rural or inaccessible regions. This study systematically assessed the available terrestrial water resources aimed at rainwater harvesting potential in a seawater-based community known as Poblacion Sitangkai, Philippines. The spatial distribution of rainwater harvesting potential was evaluated using a vector grid approach in QGIS [4],[5], providing valuable insights for sustainable water resource planning [8],[9],[10], as well as resilience against freshwater scarcity. The general objective of this study is to determine the potential for rainwater harvesting in the seawater community, mainly focused on Poblacion Sitangkai. Specifically, it aimed to determine the following: Climatological data; digitize boundary maps and vector polygons representing roof areas; estimate rainwater collection volumes; identify peak rainwater harvesting months and optimal periods for rainwater collection.

For this purpose, a vector grid approach is utilized in QGIS to determine the spatial pattern of rainwater harvesting potential over Poblacion Sitangkai, with the ultimate goal of providing data for sustainable water resource planning and vulnerability reduction against the freshwater shortage.

Scope and Limitation. Rainwater harvesting potential Poblacion Sitangkai spatial distribution vector Grid QGIS Macro grid water collection estimates were calculated monthly precipitation data from June 2023 through March 2024 except February since there was no recorded data for technical

reasons behind (Weatherlink station in Bongao, Tawi-Tawi). They were using rain data, digitizing an area of the roof to calculate its potential rainfall catchment. The study also sought to establish when rainwater harvesting peaked by linking precipitation patterns with appropriate time for maximum water collection.

Data Sources and References. These weather stations provide precipitation data from local climatological reports (Davis Instrument, Weatherlink Network). Boundary's data is from DENR (Department of Environment and Natural Resources), Region XI - CDD, OpenStreetMap. The boundaries for barangays and the island are as per references — they have been sourced from different authorities and digital platforms.

Study Area. The location of the study area is shown on a map in Fig. 1 using WGS84/UTM zone 31 N as a coordinate system; the Universal Transverse Mercator (UTM) and geodetic datum used are, respectively, UTM and World Geodetic System 1984. A map scale of 1:100,000 means one unit on the map = 100,000 units on the ground. It indicates the kind of detail and area you want to cover. These are boundaries established by the DENR Region XI - CDD, and this area was digitized using a reference boundary from OpenStreetMap for the Sitangkai Boundary. Its nine barangays are Datu Baguinda Putih, Imam Sapie, North Larap, Panglima Alari Sitangkai Poblacion South Larap Tongosung and Sipangkot

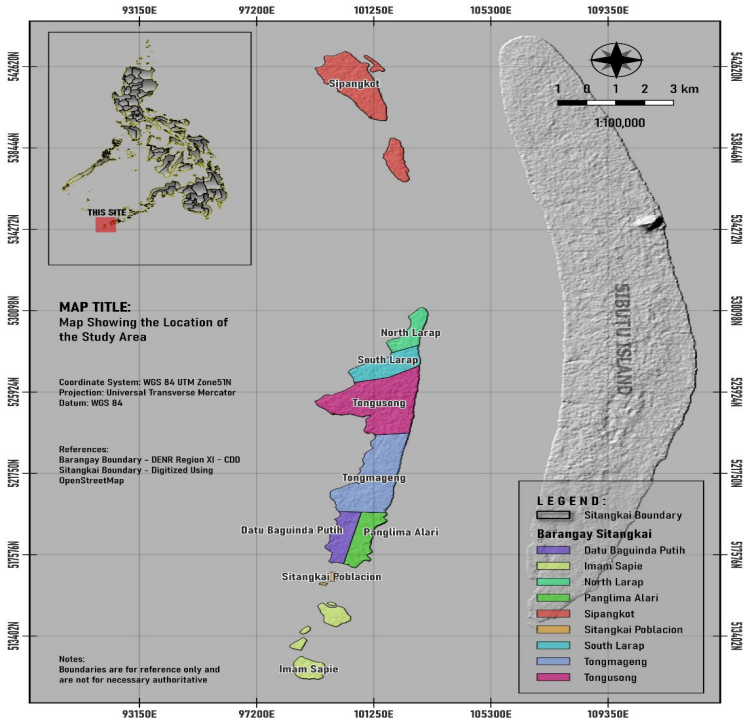

Fig. 1. Map of the study area.

Conceptual Framework. A conceptual framework for rainwater harvesting potential analysis at each step, with input-process-output Fig. 2. The steps of rainwater harvesting potential estimation consist of working out the observed precipitation data at a high density, locally relied on climatological sources, and it counts with Davis Instruments and Weatherlink Network, among others. The data are collected through local weather stations, making it accurate and relevant.

The data on regional boundaries are taken from DENR Region XI - CDD for the next step. OpenStreetMap has helped digitize this data for use as part of GIS analysis. The outcome is a digital map of the boundaries defining the object's geographical extent under discussion. All the roof areas of buildings are identified and digitized as vector polygons using GIS software within the digital boundaries. This step digitizes roof segments and makes them usable for spatial analyses. This gives a highly detailed map of vector polygons showing the exact footprints for each roof. This has to be done on top or over a grid system and the digitized roof area polygons. As a result, this process can then estimate how much rainwater could be collected depending on the size of each roof. Its results consist of a series showing the quantity of rainwater that could be collected from each respective roof

area. Correlation maps of the captured precipitation data with estimated rainwater collection volumes and maximum rainwater harvesting potential periods are determined. Analyzing these patterns allows the study to identify which months of rainwater collection would be most effective. It identifies which months to harvest the most rainwater. Lastly, the associated data is analyzed to determine when rainwater harvesting should occur for each place. This requires a step-by-step analysis of various peaks in the precipitation pattern and their corresponding alignment with volumes estimated to be collectible. The result is a list of optimal times to harvest rainwater, allowing correct utilization and maintaining water condition efficiency.

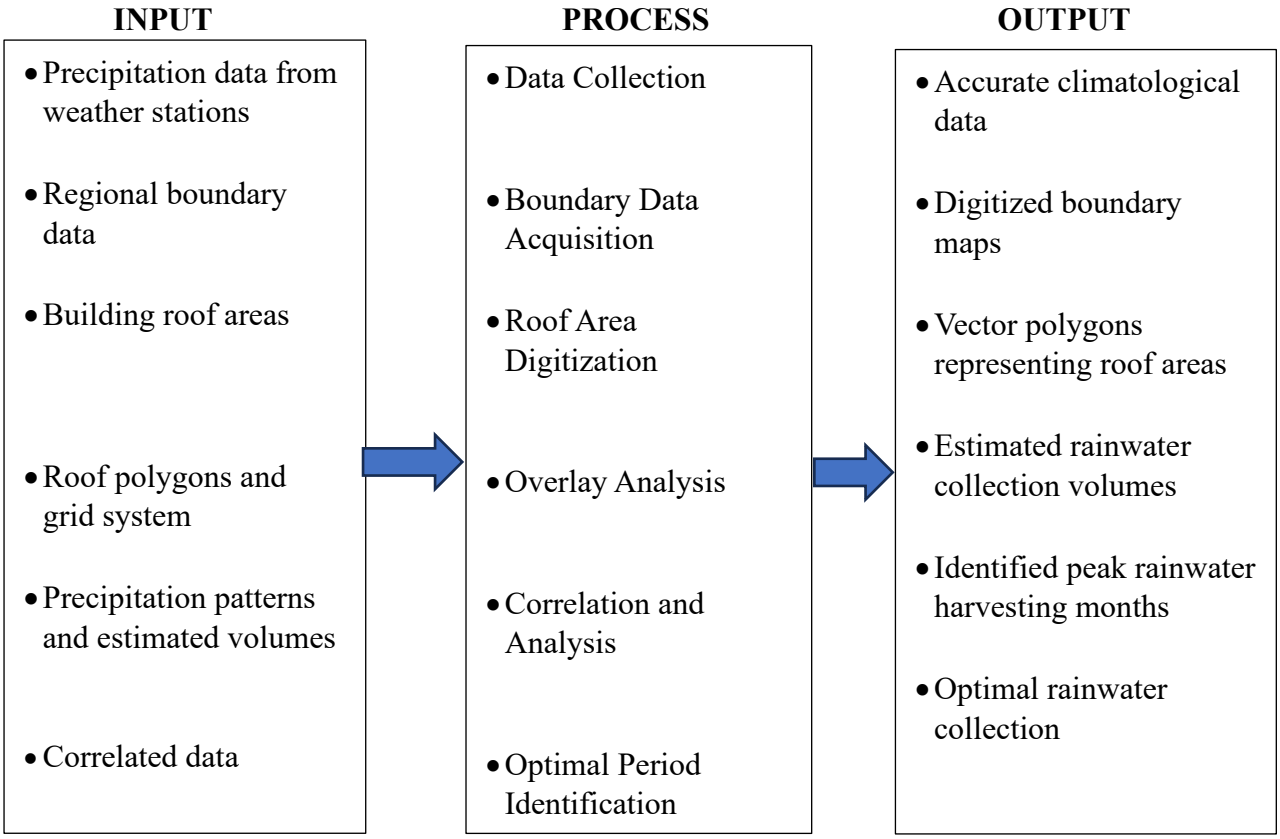

Fig. 2. Conceptual Framework.

Data Collection. This data is from local weather stations with state-of-the-art instruments, such as those made by Davis Instrument, & connected to the Weatherlink Network. These stations monitor meteorological parameters like the amount, frequency, and intensity of rainfall. The acquired information is subsequently compiled into a comprehensive data set that accurately portrays the precipitation in any given area.

Boundary Data Acquisition. The DENR Region XI – CDD provided the boundary data of the study area. This data is essential for identifying the regional borders to confine this analysis. This data is converted to digital format using OpenStreetMap, a free and open-source software tool that accurately illustrates boundaries on maps. This step involves digitizing the spatial information from physical boundaries and creating a digital map for further GIS analysis.

Roof Area Digitization. The next thing to retrieve digitalization is the roof areas of buildings within the defined boundaries by making accurate vector polygons in the form of roofs. It is done using GIS software with precise digitization. It allows the creation of vector polygons, which are digital versions of each physical roof area. The above polygons are crucial to computing rainwater harvesting capacities due to their easy recovery and quantifiable representation of the collection area.

Overlay Analysis. The first thing to do is try doing overlay analysis with the digitized roof polygons. First, make a fishnet from the roof polygons. The grid system allows the study area to be divided into regular units, helping researchers approximate volumes of rainwater that can be collected. This step aims to get an approximate amount of rainwater that we can collect for all roof areas. Overlaying the polygons over a grid allows for computing how much rainwater can be collected from each polygon for different storm events and applied to rooftop drainage areas.

Correlation and Analysis. This step combines the measured precipitation data with an estimate of rainwater collection volumes. The other describes collected precipitation data, how rainfall varies over time, and the estimated volume of rainwater that can be harvested. Analyzing these two datasets together made it possible to determine which months of the year the rainwater application would be most effective. This makes the periods with water resource rainfall potentially most significant to a regional extent, as shown by this correlation analysis.

Optimal Period Identification. Then, choose periods of rainwater collection using the correlated data. This looks at the peak harvesting months identified and then provides time slots within these months that rainwater collection would be most beneficial. This is to design rainwater harvesting (RwH) systems centered around these times, thereby harnessing the greatest efficacy and return from water catchment. The result was a schedule for the optimal times for rainwater harvesting to help design and install an appropriate collection system.

Result and Discussion

Climatological Data Analysis. In June, the map depicts several pockets with "very low" to" very high precipitation impactful zones. Most of the island is in "Very Low" to "Low" precipitation (0 - 12.12 mm), particularly central portions and parts of the northwest. This persistence results in dry conditions prevailing across these areas during June. A section in the southern coastal regions shows "Moderate" rainfall (12.13 - 18.18 mm). Known to witness marginally higher rain, this only in some of the isolated pockets, especially around the southern part near Datu Baguinda Putih and Panglima Alari in Fig. 3; area rainfall is consistently ranked as "High" or even better depending on the categorization used, i.e., "very high"(18.19 -associative estimate mean->30 mm). This may include areas with a higher topographic elevation or coastal zones where winds increase precipitation.

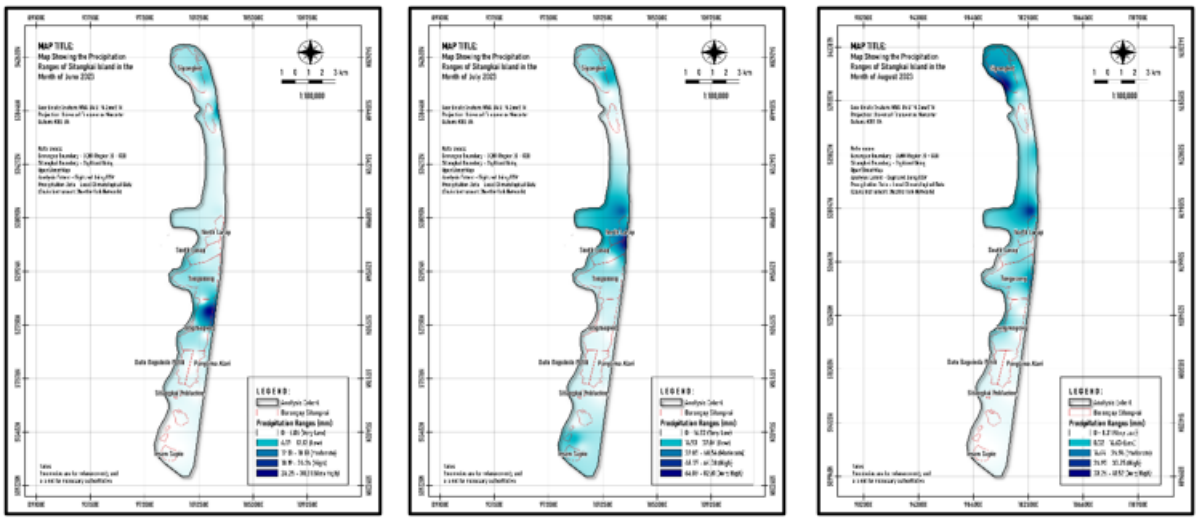

Fig. 3. Monthly Rainfall map.

The Precipitation ranges of July 2023 are categorized from very low (0 — 16.52 mm) to very high (64.09 - 82.61 mm). The island's northern part experiences more rainfall, especially in "Sipangkot" and the north coast of reps (34 km). This indicates that in July 2023, rainfall was very high to extreme. Precipitation is moderate to high in the central regions, such as "South Larap" and "Tongsung." This might also suggest a rainfall gradient, which may be governed chiefly by topographical features from elevation changes. At the same time, "Sitangkai Poblacion" and "Imam Sapie," in the southern portion, are classified as having very low to low precipitation. The wet winds from the northeast, carried by prevailing wind currents, bring air warmed up due to its increased water content over tropical seas, resulting in higher levels of precipitation on the side accordingly exposed. July is generally the wet season for this area, which adds to its already high level of rainfall.

In August 2023, precipitation levels across the island were categorized into five distinct ranges: Very Low (0 - 8.31 mm), Low (8.32 - 16.63 mm), Moderate (16.64 - 24.94 mm), High (24.95 - 33.25 mm), and Very High (33.26 - 41.57 mm). The island, characterized by its long and narrow shape, includes several named locations such as Sitangkai Poblacion, North Larap, South Larap, Tongosung, Tongmageng, Datu Baguinda Putih, Panglima Alari, and Imam Sapie. Precipitation varied significantly across the island, with the northern part near Sipangkot and the southern tip experiencing 'Very High' levels, marked by the darkest blue on precipitation maps. In contrast, the central part of the island, including areas like South Larap and Tongosung, exhibited 'Low' to 'Moderate' precipitation levels. Sitangkai Poblacion, located toward the island's southern end, was identified as being in a 'Low' precipitation zone.

From Sitangkai Island, it is expected to remain in the rainfall of September 2023. This means Very Low (0 - 14.02 mm), Low (14.03 - 28.04 mm), Moderate (28:05-42;06 mm), Dark blue shows the highest precipitation levels on the island, mainly in the southern part near Imam Sapie. The south part of Sitangkai Island, especially around Imam Sapie, saw the most precipitation in September 2023 — registering as "Very High" on this map. Such differences could be attributed to various factors such as geographical position, elevation, and weather development during that particular month. High precipitation was noted in North Larap, South Larap, Tongsung, Tongmageng, Datu Baguinda Putih Panglima Alari, and Sitangkai Poblacion. The island's northern half, where Sipangkot is located, has decreased rainfall.

Sitangkai Island October 2023 Precipitation Situation map The northern side of the island, topped by areas such as Sipangkot and North Larap, might have a reduced amount of rainfall (in both categories, "Very Low & Low" with 0 to nineteen. As we head on further southwards, the rainfall slowly rises. The rest of the island is under "Moderate" rainfall (19.41 - 29.11 mm), like in South Larap and Tongusong, both in the central part of Buayan Island. The southern part of the island, especially in Imam Sapie's neighborhood, even has a 'Very High' rainfall level (38.83 - 48.51 mm).

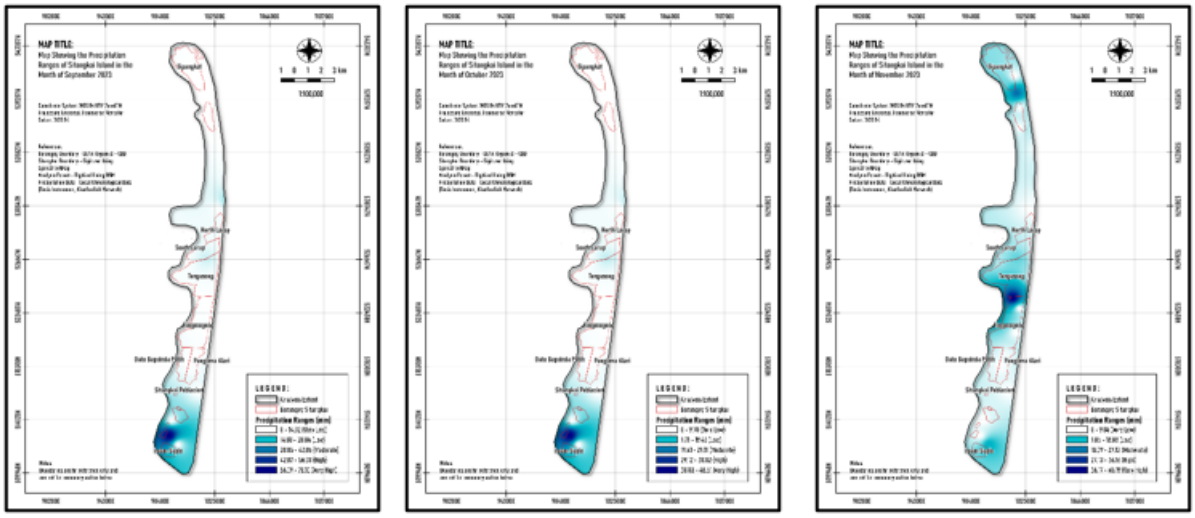

Fig. 4. Monthly Rainfall map.

This Sitangkai Island rainfall map shows the wettest and driest parts of the island in November 2023. It grades precipitation into one of five categories: Very Low (0 – 9.04 mm); Low (9.05 – 18.08 mm); Moderate (18.09-27.12 mm). Some parts of the island will be wet, others dry. More rainfall has led to increased intimidation on the island. Both the far northern and extreme southern tips of Basilan, including localities categorized as "Sipangkot," "North Larap," "Imam Sapie," and both Panglima Alari districts recorded Very Low-Low to Low levels of rainfall. Very High rain has been recorded in the central region, particularly around "Tongmageng." The precipitation is divided into five ranges, from Very Low (0.00 - 7.73 mm) to Very High (31.03 – 38.63 mm). These ranges show how wet or dry any place on the island is. This map shows the rainfall distribution on Sitangkai Island. General and abnormal rains will also increase in the island's northern part (near Sipangkot), falling from High to Very High. No continuous rainfall was recorded, while

South Larap – Tongmageng – Sitangkai Poblacion has received Moderate to High rainfall. However, as the data is for December (which may be associated with rain in this region), rainfall distribution could still make sense compared to other events at similar times. Precipitation range in Sitangkai Island for January 2024, with the thematic map visualized using different colors based on interval classification: Interval Class Very Low (0 - 0.8032 mm); Low (0.8033 - 1.6064 mm); Moderate (7-25) ranges from blue to green. The darkest colors indicate the highest precipitation levels.

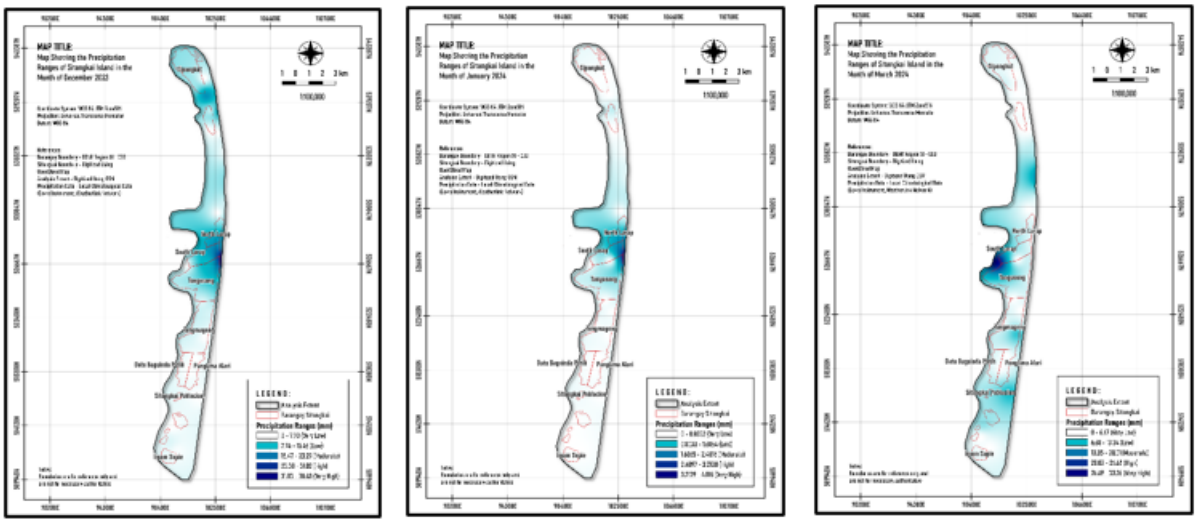

Fig. 5. Monthly Rainfall map.

Now, the 2024 Sitangkai Island March precipitation ranges await the map. Different classifications of the precipitation in 0–33.36 mm and more than 33.37 mm serve as accurate trackers of extreme rainfall events within their domains.

Monthly Rainfall Analysis. The graph illustrated that the June 2023 precipitation data shows a scattered rainfall pattern throughout the month. Most days, it doesn't have rain, but sometimes, the reality changes its mind. Most of the rain was heavy, which occurred on only four days: the 5th (up to a maximum rainfall in one day), the 14th, and the 23rd, with peaks exceeding daily values over those periods with returns up to the month as shown during violent daily events of the past two-three decades per hour. The substantial swings across these peaks and the many zero-rain days indicate a highly erratic precipitation regime. This would suggest the area had some brief, heavy showers throughout an otherwise dry period, which can be challenging regarding water-based activities that depend on regular rainfall, such as rainwater harvesting. These peaks significantly impacted the average precipitation at these higher values compared to an intervening sequence of small days. The rarity of rain events also indicates that when there was rainfall, it may not have been for prolonged periods but in short, intense bursts.

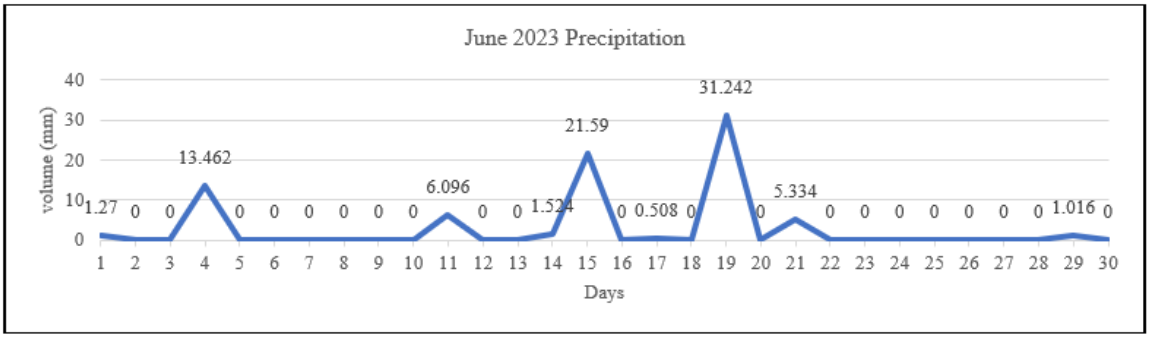

Fig. 6. Monthly precipitation trends for June.

The other process of detecting the irregular yet heavy July 2023 rainfall is to study its precipitation data. The most significant rain event happened on the 5th: a notable 86.614 mm, enough to supplement that monthly total. Following on from June, we also had some rain in July: after a wet few days to the 10th and another downpour lasting all day long on the 14th, it rained particularly

heavily again later in the month—on both the 19th—and then typically almost seven inches of rainfall (!) fell with one helluva bang overnight at half-past-three AM (or something like that), that is caused by an approaching weather front off—again—the North Atlantic—with this sudden deluge registering officially as forty-seven-point-four-nine-eight millimeters. They come after a seemingly interminable dry spell. The high rainfall on the en rue nocturnes would indicate heavy soil loading because of long, steady rains. Such episodic and intense rainfall on an ad hoc basis can pose problems for those sectors reliant on consistent rainfall; the month-to-month irregularity of precipitation this century may cause theoretically significant fluctuations in water availability.

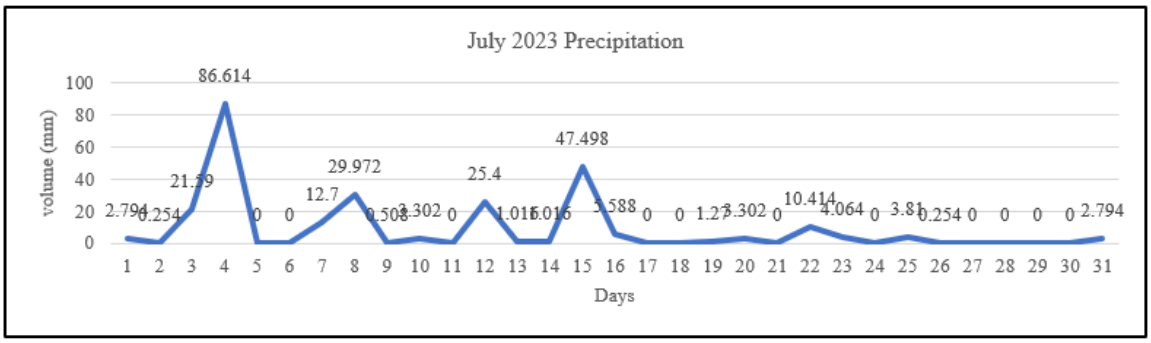

Fig. 7. Monthly precipitation trends for July.

In conclusion, the rainfall pattern performance for July complements why robust water management systems should be implemented to accommodate excess when experiencing water scarcity when experiencing water scarcity when experiencing water scarcity after-Aug23 The precipitate action distribution for domestic and export products in August 2023 strikes a diverse nature as it is scattered, with some days of drying out time to periods that have rain events at varying intensities. Significantly, the maxima of rainfall on days 9, 16, and day intervals (other) could be related to episodic weather events, possibly with storm systems transiting through this region. We see the maximum single-day rainfall at 42.672 mm on the 16th, which is high but less excessive than in July. Consecutive dry days are observed in stretches of 2 to 5 days at various points in the month, mainly during its latter half, and rain sets into some regular rhythm towards subsequently trying dates. The precipitation measures are lower than the previous month, seen from light showers and moderate rain events. This pattern will likely be less impactful on flash flooding issues than we saw in the past several months. This irregular rainfall can influence urban water reserves, reinforcing the need for flexible mechanisms that support water resource management in varying weather patterns. This month's scattered rain also requires checks and balances to ensure the viability of some projects that rely on good conditions to be successful.

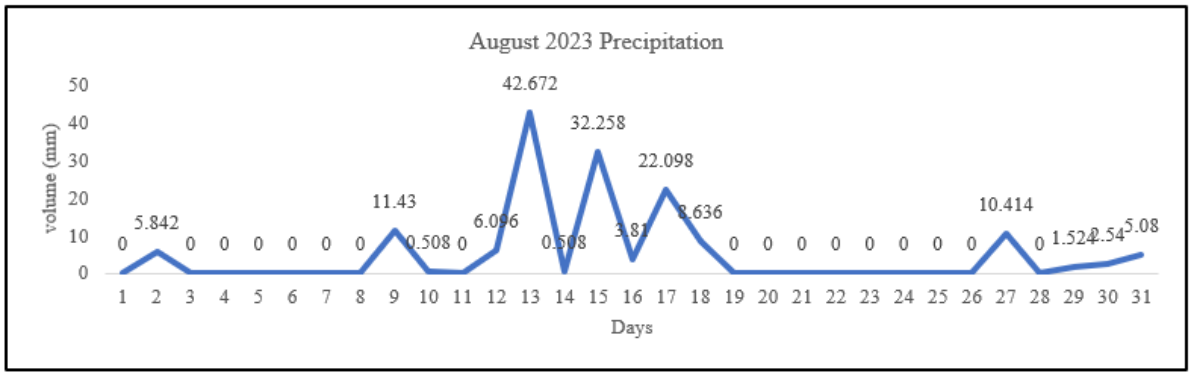

Fig. 8. Monthly precipitation trends for August.

Chart Graphic showing how September 2023 had a strange pattern where almost all days in the month got no rain. The exception to this is a distinct peak in which 70.104 mm of rainfall was logged on the 3rd, a remarkably high volume likely indicative of a significant weather event (storm). The other two light showers occurred only on the 1st (3.56 mm) and the 8th (8.89 mm). The wet day stands apart in dryness and frequency among otherwise seasonally extremely low-average days. The

pattern indicates that the water resources depend significantly on this single event, which could impact how we store and conserve water. Dry conditions for the remainder of July could strain water supplies in communities. As this precipitation pattern holds, it serves as a reminder of the unpredictable nature of weather and why food storage is essential on both ends of the spectrum.

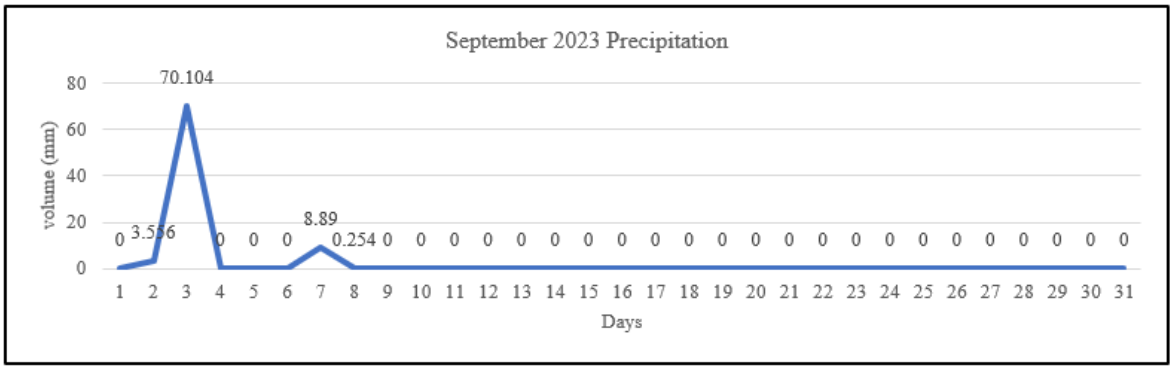

Fig. 9. Monthly precipitation trends for September.

The October precipitation data for 2023 initially suggests a substantially dry period with some exceptions in store. On the 2nd, a significant rainfall occurred, with 44.490 mm, followed by another notable rain on November 01 that registered 48.514 mm. A considerable spike in rainfall suggests a particular weather event: one hardcore storm system drenched the region with an intense deluge over two days. Afterward, things were quiet, with just a trace of rain on the 5th compared to before. There is no rain in the data for the remainder of the month, pointing to a prolonged dry spell extending into February.

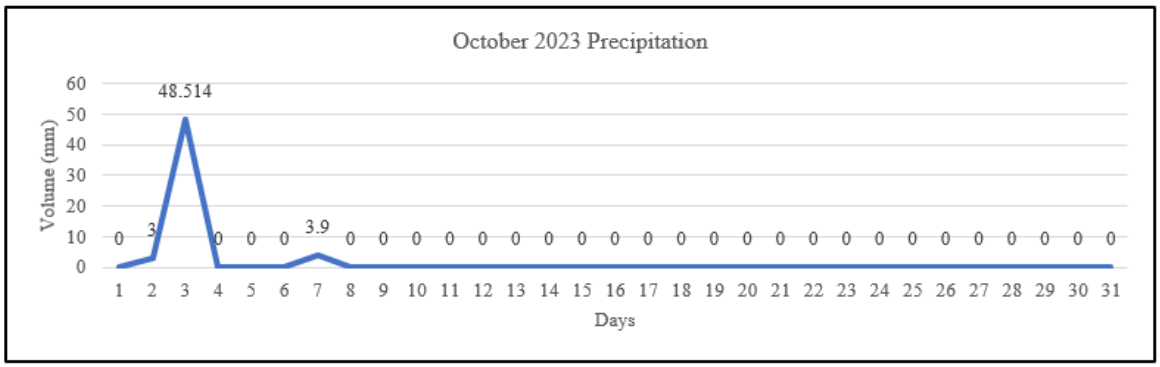

Fig. 10. Monthly precipitation trends for october.

The consequences of this pattern could vary depending on an area's water needs and climate. However, the absence of significant rain after the 5th emphasizes the need for effective water-saving measures, particularly in water management. The heavy rain at the start of the month might offer temporary relief from water shortages. Still, it also comes with risks, especially if the ground is stable from an extended dry period, meaning very little may be absorbed quickly. This stark contrast between a day of heavy rain and weeks without rainfall illustrates the challenges in managing water resources as weather patterns become more unpredictable, highlighting the importance of adaptive strategies to mitigate potential impacts on natural ecosystems and human activities.

On the other hand, the moisture graph shows a series of storms combined with gaps, probably with more improved activity than in months prior. There is rain patterned throughout the month, but on the 23rd, we have a very high record of rainfall, measured to be around 45.974 mm. Rainfall for this day in history, all years agree, displays the rainfall spike at this time and again on the 1st, 13th, 21st, 27th, and 29th, indicating variability in patterns with several separated wet periods between them. Most of these are mild to moderate showers, except near-heavy rain on the 23rd. Note that the distribution of rain during the month is better, providing some balance in water availability and usage, with caution, compared to the severe dryness experienced in previous months.

Heavy rainfall, even in the presence of a wetland, could still result in flooding if its capacity is surpassed or overwhelm roads and drains that are not designed to withstand such volumes. A few isolated extreme events cannot be ruled out during November, posing a risk for comprehensive planning and implementation at strategy and crop management levels. The long-term drought begs to be quenched by the recurring rainfall. However, spans of rainy days like last month put a final exclamation point on how much climate variability should still inform our design and infrastructure.

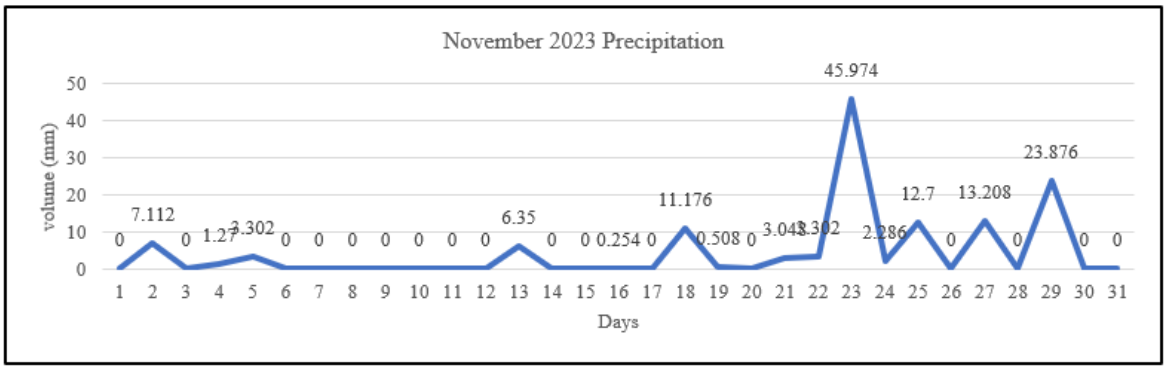

Fig. 11. Monthly precipitation trends for November.

Early in December 2023, the month hosted significant rainfall events alongside numerous dehydrated days. The relatively sharp peak on the 5th (67.818 mm) would represent a significant rainfall event, likely during a severe storm. Hence, this day accounts for the most essential proportion of immediate effects and the month's total. On the 1st, 2nd, and then on the 4th, there was a little, but not too much, with further rain (albeit lighter) bringing rainfall again on several days, including a hefty dose of nearly half an inch (12 mm) which fell as heavy showers from mid-morning into early afternoon.

The pattern for December was consistent with some rainfall events. Still, these were balanced by dry days as well, which should boost the water table without causing problems associated with prolonged heavy rainfall. However, the water management systems would have been taxed, especially as the rains on the 4th ultimately led to very high rainfall rates on the 5th, a precursor to potential flash floods. The distribution could be suitable for recharging water resources, but the variability might prompt additional management strategies to cope with drought and excess rain. This month's ups and downs in rainfall intensity emphasized the need for resilient infrastructure and flexible planning to respond to climate change.

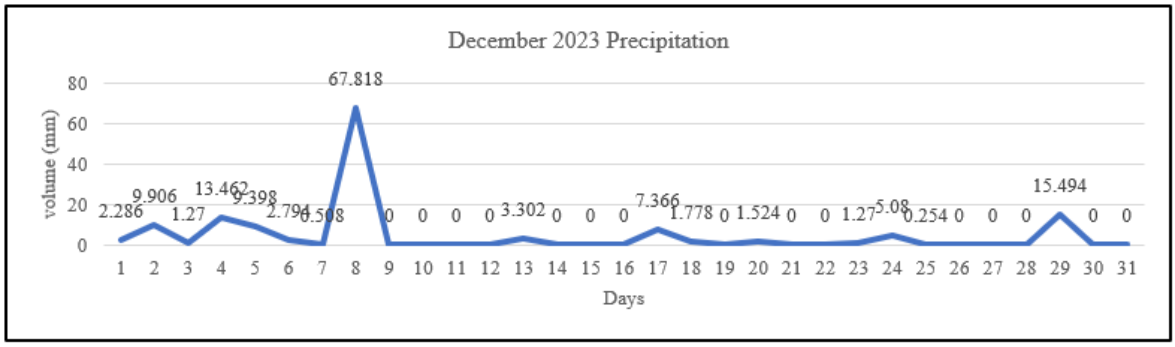

Fig. 12. Monthly precipitation trends for December.

The January 2024 precipitation chart shows a deficient, nearly non-existent rainfall for the month. The maximum rainfall recorded is on the 6th, with 7.366 mm, far short of the significant rain events in previous months. There was a slight shower on the 4th at just 1.524 mm, and a trace amount of precipitation was measured earlier in the month at 0.254 mm. The dry spell extends through the rest of the month, which could lead to drought conditions.

This prolonged absence of rain could have various implications. If January typically contributes significantly to the region's annual rainfall, water shortages could arise due to how dry this month has been. However, if this dry period occurs during an expected dry season, its impact on nearby water

resources might be less severe. The sparse rainfall events also indicate that when rain falls, more water is needed to significantly replenish systems from previous months, suggesting a tendency toward aridity or natural variability. The lesson is evident in both cases—strong water management practices are essential, and preparation for more frequent drought-like conditions may be necessary.

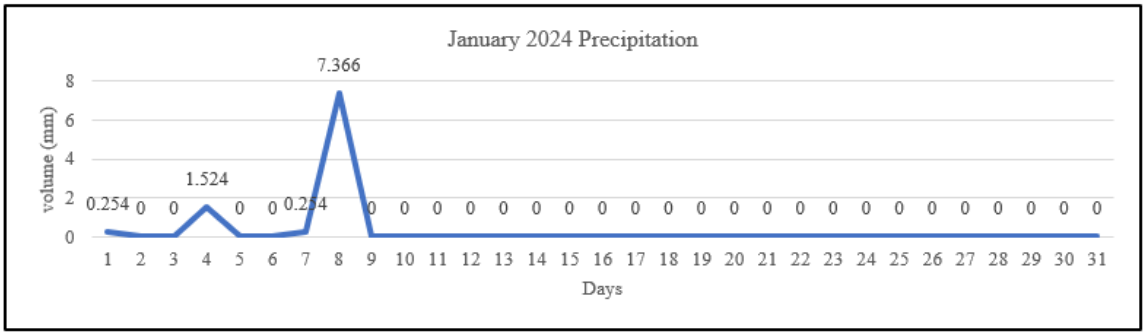

Fig. 13. Monthly precipitation trends for January.

Precipitation data for March 2024 shows the rainfall as more distributed than the dry spell seen earlier in January. Although not many, the month had some rainy days, with the most significant event on the 24th reaching 33.528 mm. This event alone contributes significantly to the month's total and likely had the most important effect on local water resources. Smaller amounts of precipitation were observed throughout the month, with a light rainfall on the 11th at 6.858 mm, followed by a moderate 16.51 mm event on the 26th, and lighter events again on the final two days, the 29th and 30th, with 7.874 mm and 4.064 mm, respectively.

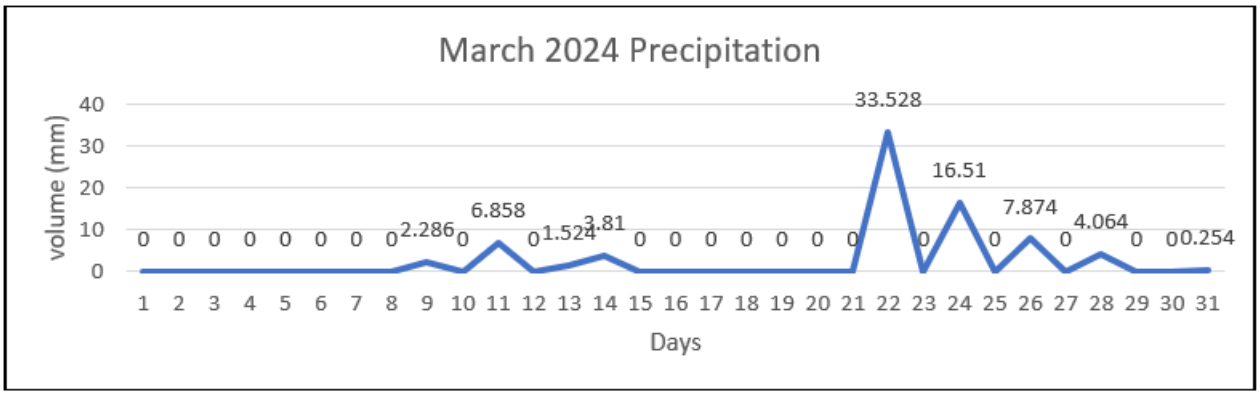

Fig. 14. Monthly precipitation trends for March.

Given the sporadic rainfall in March, we may see periods where water use is stressed between intervals of water abundance. The mid-month rainfall likely provided relief from any water deficits that had built up during the preceding and following dry days. Overall, March presented some hydrological challenges, with the prospect of ongoing dry conditions being alleviated. This mix of wet and dry spells could be exacerbated by a warming climate, leading to the need for approaches like integrated water resource management (IWRM) that promote adaptability and efficient rainwater harvesting when it does occur.

The average monthly precipitation fig. 15 for Sitangkai Island from June 2023 to March 2024 has a very pronounced seasonal characteristic, which could have significant consequences for rainwater harvesting. The peak of the rainy season in September and October reveals these as the best months to maximize water collection. With average precipitation as high as 20.7 cm, these months could fill water stores substantially if systems are adequately sized and designed for the region.

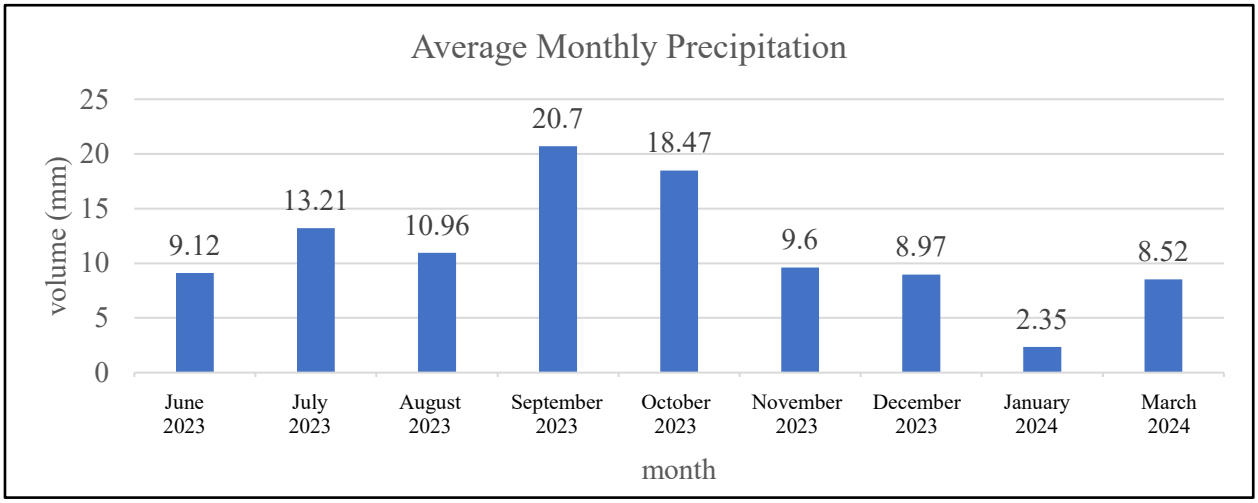

Fig. 15. Average monthly precipitation.

However, rainwater harvesting has its limitations. The 50% reduction in rainfall recorded this past January makes it an unreliable water source. This variation demands significant water storage capacity to bridge the dry periods and necessitates measures to conserve water, ensuring its utility even during extended droughts.

Historical vs. June 2023-March 2024 — Rainfall Average Comparison

NASA's POWER CERES/MERRA2 meteorological parameter data, spanning from January 01, 1981, to December 31, 2021, with native resolution (monthly and annual mean), provides a comprehensive dataset [16], [17], [18]. The coordinates are pinpointed at a latitude of 4.6615 and a longitude of 119.392. The dataset also reports an elevation average of only 0.07 meters, indicating a flat area, possibly near sea level.

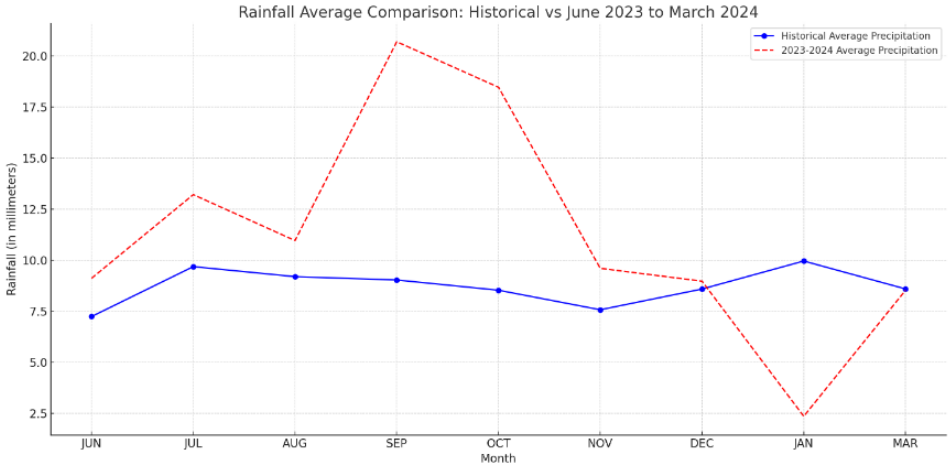

Fig. 16. Monthly Average Rainfall Historical vs. June 2023-March 2024.

The model provides parameters 10 meters above ground level (AGL) and other wind and atmospheric pressure altitudes. Wind direction is measured in degrees (up to WD10M and WD50M), offering a good characterization of the leading wind trends in the area. Wind speed is reported at 10 meters (WS10M) and 50 meters, with maximum (WS10M_MAX, WS50M_MAX), minimum (WS10M_MIN, WS50M_MIN), and range values, which are essential for examining meteorological patterns and gradients over the years.

Fig. 16 plots rainfall events for each month, comparing historical averages with actual data from June 2023 to March 2024. June 2023 rainfall is close to the expected historical value, indicating stable rainwater harvesting potential for this month. The data for July 2023 shows a slight increase over historical averages, suggesting a marginally higher potential for water collection. August 2023 also aligns closely with historical averages.

September 2023 stands out with significantly higher rainfall than average, and this trend continues into October 2023. However, rainfall in November 2023 dips slightly below the historical mean. December 2023 maintains an average rainfall, while January 2024 experiences a significant drop, far below historical averages. Fortunately, March 2024 shows a recovery, with rainfall returning closer to historical norms after the dry January.

This comparison highlights the need for flexible and adaptive rainwater harvesting strategies to manage surpluses and shortages. While some months deviate significantly from historical averages, others follow expected patterns. Planning should focus on average conditions while accounting for increasing variability and potential extremes due to climate change. These anomalies should be considered for infrastructure resilience, ensuring that rainwater harvesting systems are designed to handle the unpredictability of rainfall patterns.

Roof Area Digitization. It can be seen in Fig. 17 that data for roof areas in yellow have been gathered and digitized into vector polygons. A grid is laid on top of these roof areas, and the data in each grid cell are summarized as shown in the table below. This analysis estimates the potential capacity for rainwater harvesting by considering the roof areas within each cell and making a regression across the volume that can be collected using precipitation data. The summary table shows how the total roof area and number of houses per grid cell have been computed, which is crucial for planning rainwater harvesting capacities.

It also notes substantial heterogeneity across grids in the bar graph of Fig. 5 of the average monthly rainwater harvested per grid. This is likely due to differences in roof area—more square footage would catch more rain—or variations in geography from one rainfall pattern locality to another. These differences can highlight the potential for optimization, such as improving roof designs or maintenance operations to increase rainwater capture efficiency. A more detailed analysis of seasonal trends month-by-month may also inform the time-varying capabilities of rainwater harvesting systems, supporting policy decisions on resource management and infrastructure investments. Optimizing the use of rainwater, particularly in regions where it is scarce, supports operational improvements and advances sustainability goals.

The analysis of the annual RWH volumes in Fig. 18 demonstrates significant differences between various grids. Grid XXX has the highest annual RWH, reaching 1,748,029 liters, which is much higher than the second-ranked grid. High-potential grids ranked 2-10, show relatively high RWH performance, with volumes ranging from 1,617,698 to 942,780 liters. Mid-potential grids, ranked 11-24, have RWH volumes between 872,240 and 300,934 liters. Finally, low-potential grids, ranked 25th to 48th, show the lowest RWH volumes, ranging from 300,437 to 4,963 liters.

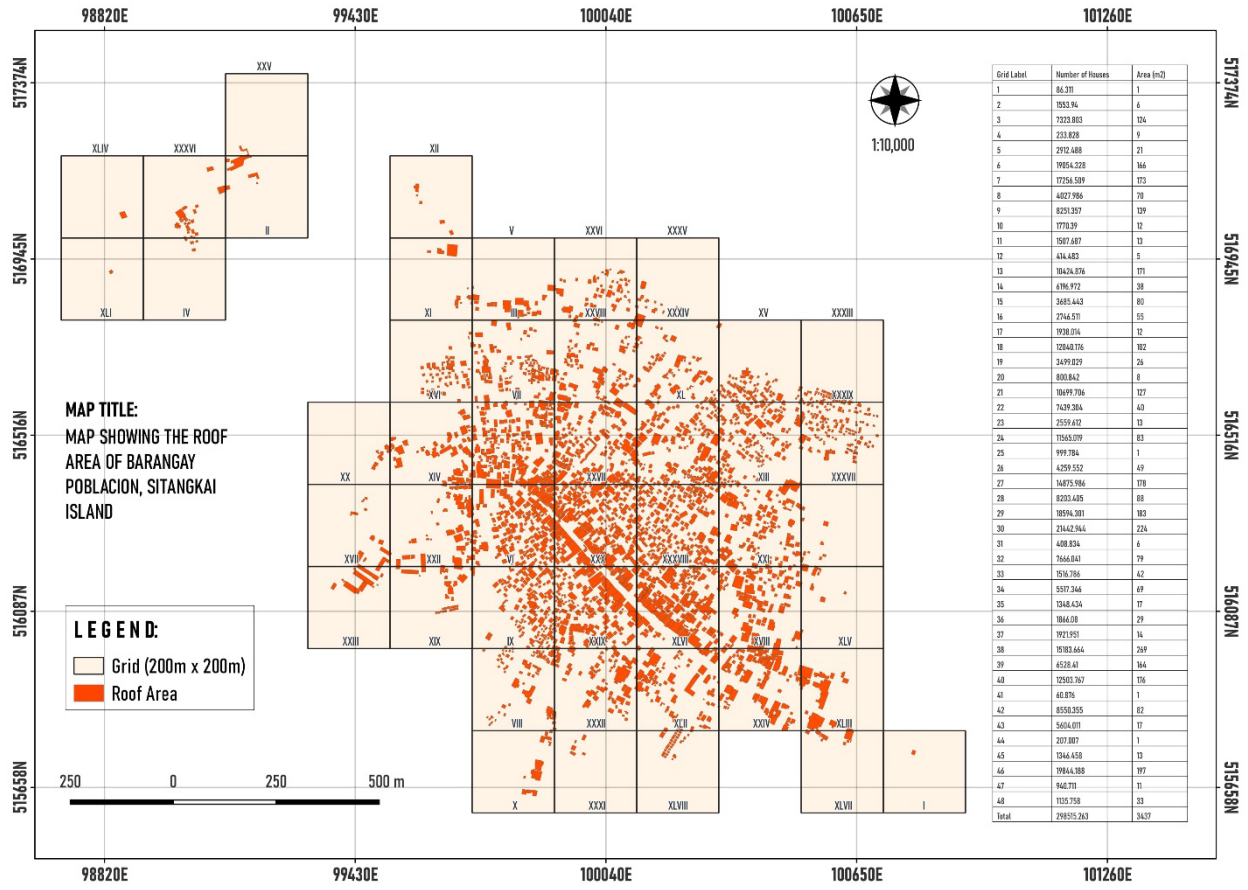

Fig. 17. Digitized roof area of 200 m x 200 m Grid.

Notably, Grid XXX and Grid XLI in Table 1 demonstrate the most significant difference, with over 1.74 million liters in the first case and less than 5,000 liters in the second. The grid volumes highlight that the top 10 grids account for most of the RWH, while the lower-ranked grids contribute relatively little.

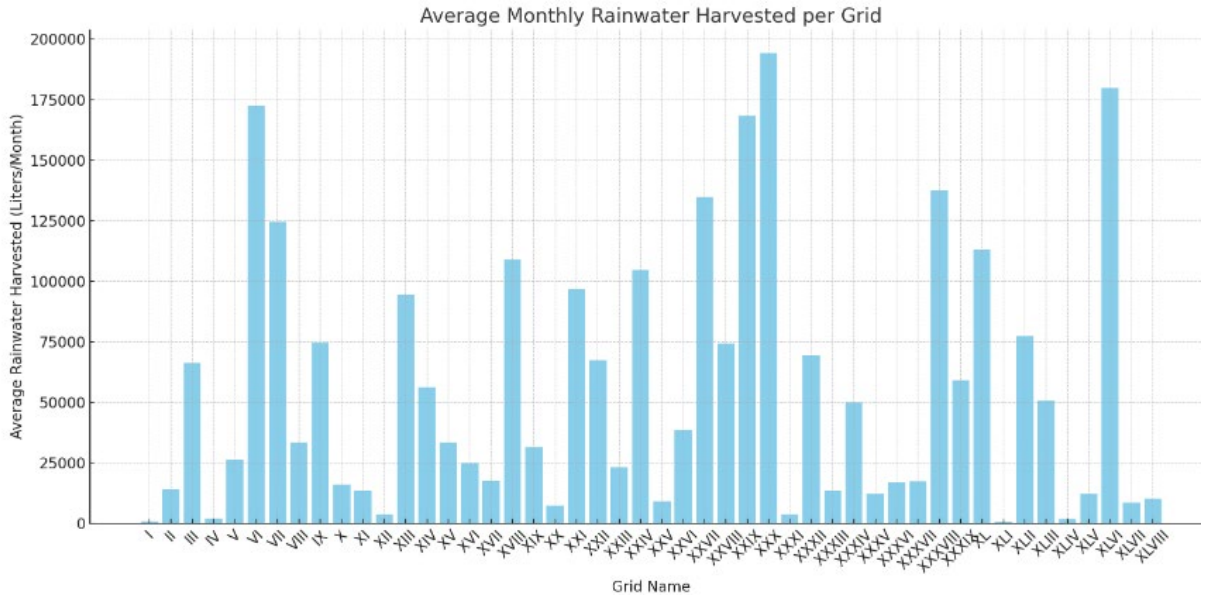

Fig. 18. Average monthly rainwater harvested per grid.

The total roof area per grid analysis indicates significant variation, likely contributing to the observed differences in annual rainwater harvesting (RWH) volumes. Grid XXX, with the most extensive roof area of 21,442.944 square meters, shows the highest potential for RWH. Other grids with large roof areas include VI (19,054.328 square meters), XLVI (19,844.188 square meters), and XXIX (18,594.301 square meters).

Table 1. Annual Rainwater Harvested Potential Per Grid (200m by 200m).

Rank	Grid Identification	Annual RWH, Liters/Year	Rank	Grid Identification	Annual RWH, Liters/Year
1	Grid XXX	1,748,029 liters	25	Grid XV	300,437 liters
2	Grid XLVI	1,617,698 liters	26	Grid XIX	284,357 liters
3	Grid VI	1,553,309 liters	27	Grid V	237,426 liters
4	Grid XXIX	1,515,807 liters	28	Grid XVI	223,896 liters
5	Grid XXXVIII	1,237,772 liters	29	Grid XXIII	208,660 liters
6	Grid XXVII	1,212,690 liters	30	Grid XVII	157,987 liters
7	Grid VII	1,122,168 liters	31	Grid XIX	284,357 liters
8	Grid XL	1,019,307 liters	32	Grid V	237,426 liters
9	Grid XVIII	981,515 liters	33	Grid XVI	223,896 liters
10	Grid XXIV	942,780 liters	34	Grid XXIII	208,660 liters
11	Grid XXI	872,240 liters	35	Grid XVII	157,987 liters
12	Grid XIII	849,836 liters	36	Grid XXXVII	156,677 liters
13	Grid XLII	697,025 liters	37	Grid XXXVI	152,123 liters
14	Grid IX	672,651 liters	38	Grid X	144,322 liters
15	Grid XXVIII	668,742 liters	39	Grid II	126,677 liters
16	Grid XXXII	624,936 liters	40	Grid XXXIII	123,648 liters
17	Grid XXII	606,452 liters	41	Grid XLVII	76,687 liters
18	Grid III	597,036 liters	42	Grid XX	65,285 liters
19	Grid XXXIX	532,196 liters	43	Grid XII	33,789 liters
20	Grid XIV	505,177 liters	44	Grid XXXI	33,328 liters
21	Grid XLIII	456,839 liters	45	Grid IV	19,062 liters
22	Grid XXXIV	449,774 liters	46	Grid XLIV -	16,875 liters
23	Grid XXVI	347,239 liters	47	Grid I	7,036 liters
24	Grid VIII	300,934 liters	48	Grid XLI	4,963 liters

Conversely, table 2 Grid I features a small roof area of 86.311 square meters, while XLIV (207.007 square meters) and XLI (60.876 square meters) have only slightly more significant areas.

These differences in roof areas account for the significant variations in RWH volumes. The best-performing grids in RWH have significantly higher roof areas, highlighting the importance of roof size in successful rainwater harvesting.

Table 2. Total Roof Area Per Grid.

Grid Name	Order	Total Roof Area (Square meter)	Grid Name	Order	Total Roof Area (Square meter)
I	1	86.311	XXV	25	999.784
II	2	1553.94	XXVI	26	4259.552
III	3	7323.803	XXVII	27	14875.986
IV	4	233.828	XXVIII	28	8203.405
V	5	2912.488	XXIX	29	18594.301
VI	6	19054.328	XXX	30	21442.944
VII	7	17256.509	XXXI	31	408.834
VIII	8	4027.986	XXXII	32	7666.041
IX	9	8251.357	XXXIII	33	1516.786
X	10	1770.39	XXXIV	34	5517.346
XI	11	1507.687	XXXV	35	1348.434
XII	12	414.483	XXXVI	36	1866.08
XIII	13	10424.876	XXXVII	37	1921.951
XIV	14	6196.972	XXXVIII	38	15183.664
XV	15	3685.443	XXXIX	39	6528.41
XVI	16	2746.511	XL	40	12503.767
XVII	17	1938.014	XLI	41	60.876
XVIII	18	12040.176	XLII	42	8550.355
XIX	19	3499.029	XLIII	43	5604.011
XX	20	800.842	XLIV	44	207.007
XXI	21	10699.706	XLV	45	1553.465
XXII	22	7439.304	XLVI	46	19844.188
XXIII	23	2559.612	XLVII	47	940.711
XXIV	24	11565.019	XLVIII	48	1135.758

Conclusion

This study emphasizes the potential of rainwater harvesting as a highly effective practice for increasing water availability, particularly for Sitangkai Island. Based on a vector grid approach in QGIS, the analysis evaluates the spatial potential for rainwater harvesting systems across nine barangays. The study suggests that potential water yield varies substantially due to differences in roof space and precipitation patterns across different geographic regions.

Future Works

In the follow-up, design optimization for roof systems will be essential to enhance rain capture on a building scale. This requires assessing harvested rainwater's monthly demand and sufficiency to ensure it meets the community's needs. Additionally, investigating the possible development of a basic rainwater collection storage system within a 200 m x 200 m grid rooftop is essential. Creating a viable storage system capable of housing the water collected from each optimized roof sector is also crucial. These research directions will contribute to a better understanding and application of rainwater harvesting as an alternative, sustainable solution for freshwater scarcity.

References

[1] D. M. Bushnell, “Halophytes/Saline Water/Deserts/Wastelands Nexus as a Scalable Climate Mitigation including Freshwater Impacts,” *Water*, vol. 16, no. 3, pp. 373–373, Jan. 2024, doi: https://doi.org/10.3390/w16030373.

[2] N. Afsari, S. B. Murshed, S. M. N. Uddin, and M. Hasan, “Opportunities and Barriers Against Successive Implementation of Rainwater Harvesting Options to Ensure Water Security in Southwestern Coastal Region of Bangladesh,” *Frontiers in Water*, vol. 4, May 2022, doi: https://doi.org/10.3389/frwa.2022.811918.

[3] P. Blanco-Gómez, C. Amurrio-Garcia, J. L. Jiménez-García, and J. M. Cecilia, “CPR Algorithm—A new interpolation methodology and QGIS plugin for Colour Pattern Regression between aerial images and raster maps,” *SoftwareX*, vol. 22, p. 101356, May 2023, doi: https://doi.org/10.1016/j.softx.2023.101356.

[4] G. W. Pereira, D. S. M. Valente, D. M. de Queiroz, A. L. de F. Coelho, M. M. Costa, and T. Grift, “Smart-Map: An Open-Source QGIS Plugin for Digital Mapping Using Machine Learning Techniques and Ordinary Kriging,” *Agronomy*, vol. 12, no. 6, p. 1350, Jun. 2022, doi: https://doi.org/10.3390/agronomy12061350.

[5] V. Saxena, P. Mundra, and D. Jigyasu, "Efficient Viewshed Analysis as QGIS Plugin," IEEE Xplore, December 01, 2020. https://ieeexplore.ieee.org/abstract/document/9362730 (accessed March 29, 2023).

[6] Kundan Dhakal, “An introduction to spatial data analysis: remote sensing and GIS with open source software. Martin Wegmann, Jakob Schwalb-Willmann, and Stefan Dech. 2020. Pelagic Publishing, Exeter, United Kingdom. 365 pp. $40.28 paperback. ISBN: 978-1-78427-213-5,” Journal of Wildlife Management, vol. 86, no. 7, Jul. 2022, doi: https://doi.org/10.1002/jwmg.22295.

[7] Kundan Dhakal, “An introduction to spatial data analysis: remote sensing and GIS with open source software. Martin Wegmann, Jakob Schwalb-Willmann, and Stefan Dech. 2020. Pelagic Publishing, Exeter, United Kingdom. 365 pp. $40.28 paperback. ISBN: 978-1-78427-213-5,” Journal of Wildlife Management, vol. 86, no. 7, Jul. 2022, doi: https://doi.org/10.1002/jwmg.22295.

[8] A. L. Muller, O. J. Gericke, and J. P. J. Pietersen, “Methodological approach for the compilation of a water distribution network model using QGIS and EPANET,” Journal of the South African Institution of Civil Engineering, vol. 62, no. 4, pp. 32–43, Dec. 2020, doi: https://doi.org/10.17159/2309-8775/2020/v62n4a4.

[9] L. Raimondi, G. Pepe, M. Firpo, D. Calcaterra, and A. Cevasco, “An open-source and QGIS-integrated physically based model for spatial prediction of rainfall-induced shallow landslides (SPRIn-SL),” *Environmental Modelling & Software*, p. 105587, Nov. 2022, doi: https://doi.org/10.1016/j.envsoft.2022.105587.

[10] D. Kumar, A. Dhaloiya, A. S. Nain, M. P. Sharma, and A. Singh, “Prioritization of Watershed Using Remote Sensing and Geographic Information System,” *Sustainability*, vol. 13, no. 16, p. 9456, Aug. 2021, doi: https://doi.org/10.3390/su13169456.

[11] D. Kumar, A. Dhaloiya, A. S. Nain, M. P. Sharma, and A. Singh, “Prioritization of Watershed Using Remote Sensing and Geographic Information System,” *Sustainability*, vol. 13, no. 16, p. 9456, Aug. 2021, doi: https://doi.org/10.3390/su13169456.

[12] J. Pérez-Padillo, J. G. Morillo, E. C. Poyato, and P. Montesinos, “Open-Source Application for Water Supply System Management: Implementation in a Water Transmission System in Southern Spain,” *Water*, vol. 13, no. 24, p. 3652, Dec. 2021, doi: https://doi.org/10.3390/w13243652.

[13] Wilian Rodrigues Ribeiro *et al.*, "Water demand of central pivot-irrigated areas in Bahia, Brazil: management of water resources applied to sustainable production," vol. 24, no. 10, pp. 12340–12366, Nov. 2021, doi https://doi.org/10.1007/s10668-021-01950-8.

[14] A. Alamanos and S. Linnane, "Estimating SDG Indicators in Data-Scarce Areas: The Transition to the Use of New Technologies and Multidisciplinary Studies," *Earth*, vol. 2, no. 3, pp. 635–652, Sep. 2021, doi: https://doi.org/10.3390/earth2030037.

[15] K. F. Darweesh et al., "Three decades of remote sensing habitat mapping, along the Egyptian Coast of Aqaba Gulf, Red Sea," *Egyptian Journal of Aquatic Biology and Fisheries*, vol. 25, no. 6, pp. 467–487, Dec. 2021, doi: https://doi.org/10.21608/ejabf.2021.214042.

[16] M. Shamkhi, A. Jawad, and T. Jameel, "Comparison between Satellite Rainfall Data and Rain Gauge Stations in Galal-Badra Watershed, Iraq," Oct. 2019, doi: https://doi.org/10.1109/dese.2019.00069.

[17] T.T.B. Valeriano, G. de Souza Rolim, R.C. Bispo, J. R. da Silva Cabral de Moraes, and L.E. de O. Aparecido, "Evaluation of air temperature and rainfall from ECMWF and NASA gridded data for southeastern Brazil," *Theoretical and Applied Climatology*, vol. 137, no. 3–4, pp. 1925–1938, Nov. 2018, doi: https://doi.org/10.1007/s00704-018-2706-z.

[18] S. Ali, Z. T. Xu, M. Henchirli, K. Wilson, and J. Zhang, "Studying of drought phenomena and vegetation trends over South Asia from 1990 to 2015 by using AVHRR and NASA's MERRA data," *Environmental Science and Pollution Research*, vol. 27, no. 5, pp. 4756–4768, Dec. 2019, doi: https://doi.org/10.1007/s11356-019-07221-4.